Strain Effects in the Mass Flux of Methanol in Poly(methyl Methacrylate)*

ROBERT A. WARE and CLAUDE COHEN, *School of Chemical Engineering, Cornell University, Ithaca, New York 14853*

Synopsis

Diffusion of organic solvents into glassy polymers often results in a phase transformation of the hard, solid polymer into a swollen, rubbery material. During the sorption, internal stresses exist in the swollen and glassy parts of the polymer and are thought to contribute significantly to the "anomalous" diffusion observed in many penetrant–polymer systems. In this investigation, isothermal sorption data for the methanol–poly(methyl methacrylate) system have been obtained on plates ranging in thickness from $\frac{1}{32}$ to $\frac{1}{4}$ in. The results show features characteristic of both a strain-dependent diffusion coefficient and of a stress gradient contribution to the mass flux. An attempt to reproduce these results by combining a strain-dependent diffusion coefficient model with a stress-induced contribution to the flux is presented.

INTRODUCTION

The diffusion behavior of many organic solvents in glassy polymers cannot be described adequately by Fick's law with a concentration-dependent diffusion coefficient. The sorption process is complicated by the relaxation motion of the polymer in response to swelling stresses that are created as penetrant enters the polymer network. Internal stress gradients can often be as important as concentration gradients in controlling the mass flux. Several attempts have been made to model the wide range of "anomalous" behavior observed, but there has yet to be a single successful representation of all non-Fickian behavior. A recent paper by Petropoulos and Roussis[1] reviews the various proposed models to date; only those relevant to us here will be discussed briefly.

Crank's pioneering models[2] showed that anomalous diffusion in polymeric plates as exhibited by sigmoidal-shaped sorption curves may be due to different physical phenomena leading to distinct characteristics of these mass uptake curves. By introducing a time-dependent diffusion coefficient where the time dependence is due to structural relaxation of the polymer molecules accommodating the penetrant molecules, Crank obtains sorption curves, M_t/M_∞ vs. $t^{1/2}/2L$, that are sigmoidal and nonsuperimposable for different plate thicknesses (similar to the curves presented in Fig. 1). Here M_t is the mass of penetrant sorbed per mass of dry polymer at time, t, M_∞ is the equilibrium value of M_t at saturation, and $2L$ is the thickness of the plate. In this model, when M_t', the mass uptake per unit area perpendicular to the flux, is plotted versus the square root of time, $t^{1/2}$, the curves are superimposable up to their saturation level (unlike the curves of Fig. 2). On the other hand, Crank also developed a second model[2] based on a strain-dependent diffusion coefficient which led to characteristics of the sigmoidal sorption curves opposite to those obtained above; namely, that

* Presented at the AIChE 87th National Meeting in Boston, August 20–22, 1979.

Journal of Applied Polymer Science, Vol. 25, 717–729 (1980)

0021-8995/80/0025–0717$01.30

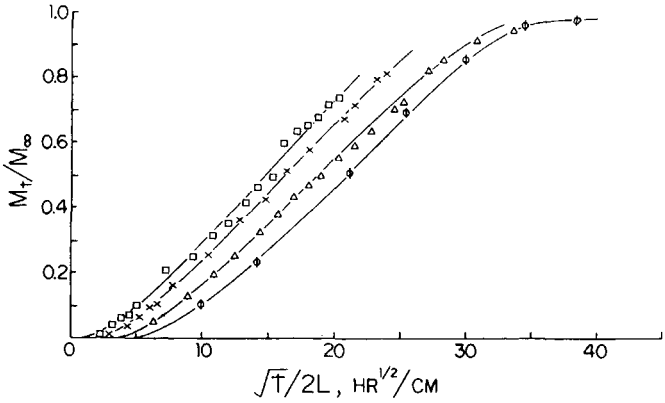

Fig. 1. Sorption curves for methanol in PMMA at 42°C for plates of thicknesses $2L$ = 0.071 cm (1/32 in.) (φ); $2L$ = 0.318 cm (1/8 in.) (△); $2L$ = 0.476 cm (3/16 in.) (×); and $2L$ = 0.635 (1/4 in.) (□).

plots of M_t/M_∞ vs. $t^{1/2}/2L$ for various thicknesses coincide (unlike those of Fig. 1) but that plots of M_t' vs. $t^{1/2}$ do not coincide and are similar to those of Figure 2. This second model is based on the postulate that compressive forces (caused by the inner glassy core) on the swollen region lead to a decrease of the diffusion coefficient in that region below its unstrained value, whereas tensile forces (caused by the swelling outer region) on the glassy unattacked core increase the diffusion coefficient in this region above its unstrained value. This model leads to the interesting prediction that at short times a thinner plate absorbs more penetrant per surface area than a thicker plate. Such an effect has been observed experimentally with methylene chloride/cellulose acetate[3] and methylene chloride/polystyrene[4] and also occurs with methanol/poly(methyl methacrylate) as exhibited by our data shown in Figure 2.

An extreme case of anomalous behavior in which the mass uptake is totally controlled by the stress gradient owing to swelling rather than by the concentration gradient is referred to as case II transport.[5] Here, the mass uptake is

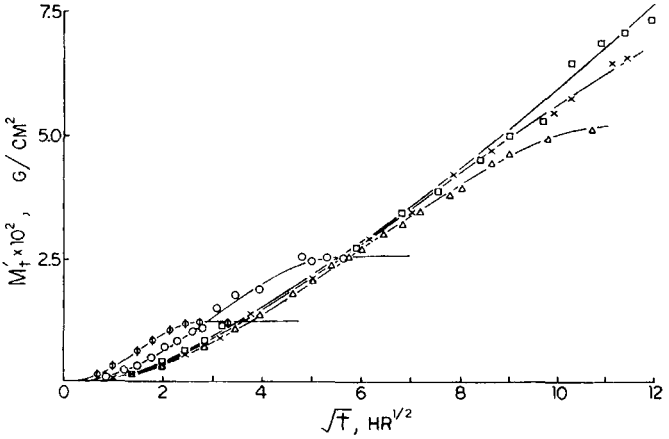

Fig. 2. Mass uptake per unit area vs. $t^{1/2}$ for methanol in PMMA at 42°C for plates of thicknesses $2L$ = 0.071 cm (1/32 in.) (φ); $2L$ = 0.147 cm (1/16 in.) (○); $2L$ = 0.318 cm (1/8 in.) (△); $2L$ = 0.476 cm (3/16 in.) (×); and $2L$ = 0.635 (1/4 in.) (□).

directly proportional to t (rather than $t^{1/2}$ for Fickian diffusion), and the swollen region is separated from the glassy inner core by a sharp concentration front that advances at constant velocity. This led several investigators[6–9] to propose a combination of Fickian diffusion and case II mechanisms to describe anomalous behavior. Thus, Frisch, Wang, and Kwei[6,7] develop the following equation for the concentration in the polymer sheet,

$$\frac{\partial C}{\partial t} = \frac{\partial}{\partial x}\left(D\frac{\partial C}{\partial x} - vC\right) \tag{1}$$

where the contributions to the flux include the usual Fickian diffusive term and a convective (case II type) term; on the other hand, Hopfenberg and his coworkers[8,9] follow the empirical approach of adding up the mass uptake owing to each of the two limiting cases, each multiplied by a different weighting factor, to account for the total mass uptake.

The solution of eq. (1) with constant D, v, and saturated surface concentration yields plots of M_t/M_∞ vs. $t^{1/2}/2L$ with similar characteristics to Crank's time-dependent diffusion coefficient model, i.e., curves that are sigmoidal in shape and thickness dependent. Other models[10] have also led to these characteristics; the advantage of eq. (1), however, is that it is based on a model of a stress-induced mass flux and is therefore amenable to matching with Crank's strain-dependent diffusion coefficient. The latter is *unique* in yielding results of the type shown in Figure 2. Furthermore, eq. (1) is able to predict, in a limiting case, the sharp concentration profile observed experimentally.[11,12] An attempt to interpret our experimental results of methanol uptake in PMMA plates of different thicknesses at 42°C with either eq. (1) or Crank's strain-dependent diffusion coefficient *alone* failed because our data, presented under Experimental Results, contained characteristics of both models. A combination of the two models that reproduces the features of our experimental results is presented under Interpretation and Analysis of Data.

EXPERIMENTAL RESULTS

Cast poly(methyl methacrylate) sheets (Plexiglas G) with nominal thickness of 1/32, 1/16, 1/8, 3/16, and 1/4 in. were used in this study. The weight-average molecular weight of the polymer as quoted from the manufacturer's specifications[13] was in the range of 1–3 million, and its density was 1.19 g/cm^3. The sheets were cut into small plates with an edge area approximately 10% of the total exposed surface area. Such a ratio has been found adequate in assuming infinite slab geometry.[11] All plates were annealed at ~100°C for two days and then weighed and maintained at the bath temperature (42°C) for a few hours before immersion into the methanol bath. Reagent-grade methanol was used without further treatment. After immersion and at successive time intervals, samples were removed from the bath, quickly wiped, and weighed in stoppered containers. A different sample was used for each point on the weight gain plots.

The weight gain data are presented in two ways. In Figure 1 plots of M_t/M_∞, where M_t is the mass of methanol sorbed per mass of dry PMMA at time t and M_∞ is its equilibrium value determined to be 0.29 at 42°C, versus $t^{1/2}/2L$ are presented. The lines through the experimental points in this figure are drawn only through the points to put in evidence the anomalous behavior of CH_3OH/

PMMA. The curves clearly display the characteristic sigmoidal shape and the rate of mass uptake dependence on the plate thickness. In Figure 2 the mass sorption data are presented in a different form; namely, the mass M_t' of methanol sorbed per unit surface area of the plate is plotted versus $t^{1/2}$. M_t' is simply related to M_t and the half-thickness of the plate by

$$M_t' = M_t \rho_p L$$

where ρ_p is the polymer density. Plates below $\frac{1}{8}$ in. thick sorbed methanol at a faster rate than the thicker ones until their saturation was reached. The three thickest plates investigated with thicknesses $2L$ equal to $\frac{1}{8}$ in. (0.318 cm), $\frac{3}{16}$ in. (0.476 cm), and $\frac{1}{4}$ in. (0.635 cm) followed the *same* sorption curve (within experimental error) up to their respective saturation level. These results indicate, and so does the theoretical prediction based on a strain-dependent diffusion coefficient, that the additional mass uptake per surface area due to this effect is relatively larger for thinner plates and disappears for thicker plates. In terms of the strain-dependent diffusion coefficient model, this is due to the fact that the largest contribution of this effect appears near saturation [when the fronts are close, see eq. (11)], at which time the mass sorbed by the thicker plates is already quite large and this effect is negligible. From the curves of Figure 2 it can be seen that the additional uptake is largest near saturation, and a simple calculation based on the additional uptake of the thinnest plate shows that for the three thickest plates examined, the contribution due to this effect will indeed be comparatively very small.

We attempted to fit our experimental data to the solution of eq. (1) with the average diffusion coefficient D and the front velocity v as parameters. The equation could describe the data for each plate thickness reasonably well, as shown in Figure 3. The slight deviation at short times, noticeable for all plates, is possibly due to the surface attaining the equilibrium concentration after some polymer relaxation[10] rather than instantaneously as modeled here. Similar

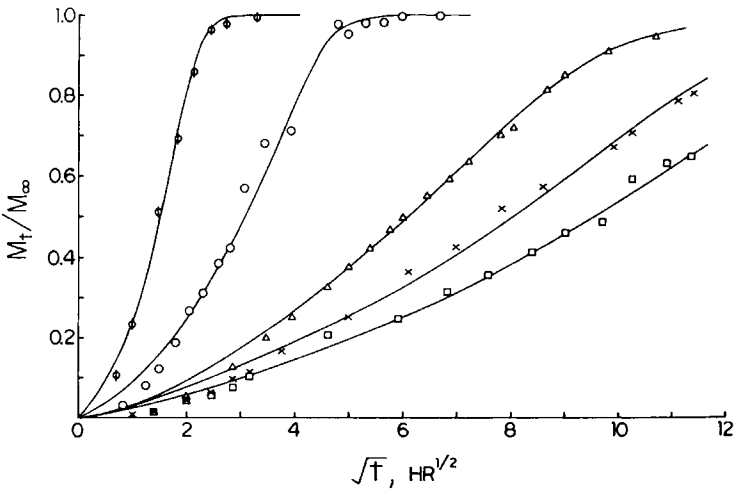

Fig. 3. Comparison of experimental sorption curves with theoretical curves obtained from eq. (1) using "best fit" value of the diffusion coefficient D and the front velocity v for $2L$ = 0.071 cm ($\frac{1}{32}$ in.) (φ); $2L$ = 0.147 cm ($\frac{1}{16}$ in.) (○); $2L$ = 0.318 cm ($\frac{1}{8}$ in.) (△); $2L$ = 0.476 cm ($\frac{3}{16}$ in.) (x); and $2L$ = 0.635 cm ($\frac{1}{4}$ in.) (□). Fitted values of D and v for each plate appear in Table I.

success with this equation has been obtained by others with the methyl acetate/PMMA[14] and acetone/poly(vinyl chloride)[15] systems. These studies, however, did not attempt experiments with different size plates. Listed in Table I is a summary of the values of D and v obtained for the various plate thicknesses of the methanol/PMMA system investigated here. The large discrepancies in the values of D and v required to fit the different sets of data are far from satisfactory since these parameters were expected to be independent of plate thickness. For the 1/32-in. plate the best fit (Fig. 3) was obtained with $D = 7.19 \times 10^{-9}$ cm^2/sec and $v = 3.83 \times 10^{-6}$ cm/sec, whereas for the 1/8-in. plate $D = 1.85 \times 10^{-8}$ cm^2/sec and $v = 8.75 \times 10^{-7}$ cm/sec. These discrepancies for the three thinnest plates, 1/32, 1/16, and 1/8 in., as indicated in Table I, were to be expected since eq. (1) leads to superimposed plots of M_t' vs. $t^{1/2}$ for the same value of D and v as opposed to the nonsuperimposable experimental results shown in Figure 2. Even when polymer swelling and an exponential concentration dependence of the diffusion coefficient are introduced into eq. (1), similar results are obtained. On the other hand, the three thickest plates, 1/8, 3/16, and 1/4 in., could be fit with values of D and v which were comparable (see Table I). Again, this is to be expected since the M_t' vs. $t^{1/2}$ data for these plates followed the same curve. Therefore, above a certain thickness, the equation proposed by Frisch et al. with a constant D and v is adequate in predicting mass uptake results. Experiments with relatively thin plates carried out in this study show the limitations of the equation.

INTERPRETATION AND ANALYSIS OF DATA

Development of the Model

The mass uptake results of the methanol/PMMA system presented above show features of both a strain-dependent diffusion coefficient and of a stress-induced flux. To reproduce these results starting from a concentration equation, both of these effects must therefore be incorporated. We develop below a modification of eq. (1) which takes into account polymer swelling and a strain-dependent diffusion coefficient. In some respect our approach resembles the rigorous extension of Crank's model due to Petropoulos and Roussis[16] but avoids the complication of having two coupled differential equations to solve, one for the concentration and the other for the stress.

By defining the position variable ξ in the polymer frame of reference[17] and redefining the diffusion coefficient and front velocity in this new frame of reference, it is possible to account for polymer swelling in the direction of penetrant

TABLE I
Values of the Diffusion Coefficient and Front Velocity Obtained from Fitting the Solution of Eq. (1) to the Methanol/PMMA Results at 42°C

Plate $2L$, in.	$2L$, cm	D, cm^2/sec	v, cm/sec
1/32	0.071	7.19×10^{-9}	3.83×10^{-6}
1/16	0.147	8.42×10^{-9}	1.92×10^{-6}
1/8	0.318	1.85×10^{-8}	8.75×10^{-7}
3/16	0.476	2.07×10^{-8}	7.97×10^{-7}
1/4	0.635	2.50×10^{-8}	7.75×10^{-7}

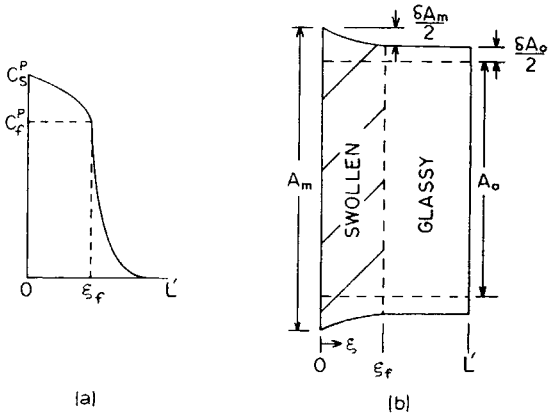

Fig. 4. (a) Schematic representation of concentration profile in the polymer plate showing penetrant front position at ξ_f separating the swollen and glassy regions. (b) Model representation of the polymer cross-sectional area during sorption showing the penetrant front at ξ_f and regions of compression and extension in the swollen and glassy polymer, respectively.

flow while still maintaining the concentration equation in the form

$$\frac{\partial C^p}{\partial t} = \frac{\partial}{\partial \xi}\left[D^p \frac{\partial C^p}{\partial \xi} - v^p C^p\right] \tag{2}$$

where the position in the polymer frame of reference is directly related to the position in the laboratory frame of reference (see Appendix). In eq. (2), the concentration C^p is expressed in terms of mass of penetrant per mass of polymer, and D^p and v^p are the diffusion coefficient and front velocity in the polymer frame of reference.* The plate thickness $2L'$ in the polymer frame of reference is expressed in terms of the total polymer mass and is therefore constant.

The problem is then to obtain the functional form of the space and time dependence of the diffusion coefficient through its strain dependence. To do this, we express the diffusion coefficients D_{sw}^p and D_c^p in the swollen and glassy regions in the form[2]

$$D_{sw}^p = D_m^p\left[1 - \mu_m \frac{\delta A_m(\xi,\xi_f)}{A_m}\right] \qquad 0 \le \xi \le \xi_f \tag{3}$$

$$D_c^p = D_0^p\left[1 + \mu_0 \frac{\delta A_0(\xi_f)}{A_0}\right] \qquad \xi_f < \xi \le L' \tag{4}$$

It is assumed that the front position, ξ_f, defined at an arbitrary but constant concentration, C_f^p, to be specified later, separates the swollen and glassy region, see Figure 4(a). Equations (3) and (4) imply a step concentration dependence of the diffusion coefficient with D_0^p as the unstrained value of D^p at low concentrations in the glassy core, and D_m^p the average unstrained value of D^p in the swollen region at high concentrations. The local (position dependent) strain in the swollen region is $\delta A_m/A_m$ and that in the core region is $\delta A_0/A_0$, where A_m and A_0 represent the unstrained surface areas of the swollen and glassy region,

* It can be shown that the relations between the diffusion coefficient and front velocity in the polymer and laboratory frames of reference are given by $D^p = \phi_p^2 D$ and $v^p = \phi_p v$, where ϕ_p is the polymer volume fraction.

respectively, see Figure 4(b). The constant μ values in eqs. (3) and (4) are proportionality factors which determine the magnitude of the strain influence on the diffusion coefficients.

Unlike Crank's original model,[2] the strain in the swollen region is taken to be position dependent in a manner consistent with the stress that induces the convective term $v^p C^p$ in eq. (2). Thus, to obtain the position dependence of the strain, we write that the stress (and also the strain, assuming Hooke's law is valid) is proportional to the total uptake of penetrant,[6]

$$S(\xi) \sim \int_0^{\xi} C^p(\xi',t)d\xi' \tag{5}$$

Equation (5) implies that at $\xi = 0$ there is no strain and the area at $\xi = 0$ must therefore be taken at its mean unstressed value of A_m, Figure 4(b). The area A_m in the swollen region in the absence of stresses is taken to be proportional to the mean concentration, C_m^p, in that region, such that

$$A_m - A_0 = (A_s - A_0)\frac{C_m^p}{C_s^p} \tag{6}$$

where A_s is the stress-free area corresponding to a uniform saturation concentration C_s^p, and A_0 is the initial area of the dry polymer which is also the stress-free area of the glassy core assumed to contain a negligible amount of penetrant. For simplicity, we take the mean concentration C_m^p of the swollen region to be $(C_f^p + C_s^p)/2$ and the area $A(\xi,\xi_f)$ in that region to vary linearly with ξ from its uncompressed state A_m at $\xi = 0$ to a maximum compression $A(\xi_f)$ at the front, see Figure 4(b). The compression of the swollen region may then be written as

$$\delta A_m(\xi,\xi_f) = A_m - A(\xi,\xi_f) = [A_m - A(\xi_f)]\frac{\xi}{\xi_f} = \delta A_m(\xi_f)\frac{\xi}{\xi_f} \tag{7}$$

The local strain in the swollen region is then given by

$$\frac{\delta A_m(\xi,\xi_f)}{A_m} = \frac{\delta A_m(\xi_f)}{A_m}\frac{\xi}{\xi_f} \tag{8}$$

whereas the spatially uniform strain in the glassy core is $\delta A_0(\xi_f)/A_0$. The area at the front, $A(\xi_f)$, which increases as the front proceeds into the polymer, is also the area of the glassy core. It is determined by a balance of the compression and extension forces expressed by[2]

$$\int_0^{\xi_f} E_m \frac{\delta A_m(\xi_f)}{A_m}\frac{\xi}{\xi_f}\,d\xi = \int_{\xi_f}^{L'} E_c \frac{\delta A_0(\xi_f)}{A_0}\,d\xi \tag{9}$$

where E_m and E_c are the Young's moduli for the swollen and glassy polymers assumed to be constant. The solution of eq. (9) combined with the fact that at $\xi = \xi_f$ the area in the swollen region is equal to that of the glassy core,

$$A(\xi_f) = A_m - \delta A_m(\xi_f) = A_0 + \delta A_0(\xi_f) \tag{10}$$

yields in a straightforward manner the following results for the two strains:

$$\frac{\delta A_0(\xi_f)}{A_0} = \left[\frac{A_m}{A_0} - 1\right]\left[1 + \frac{E_c A_m}{E_m A_0}\left(\frac{L' - \xi_f}{\xi_f/2}\right)\right]^{-1} \tag{11}$$

and

$$\frac{\delta A_m(\xi,\xi_f)}{A_m} = \left[\frac{A_m - A_0 - \delta A_0(\xi_f)}{A_m}\right]\frac{\xi}{\xi_f} \tag{12}$$

Expressions (11) and (12) along with eqs. (3) and (4) provide all the requirements for the solution of the concentration equation, eq. (2), with a strain-dependent diffusion coefficient. This has been carried out assuming a constant surface concentration C_s^p and a constant front velocity v^p using an explicit finite difference technique. At each time step the front position was located at the point where the concentration was C_f^p, the calculation of the strains and diffusion coefficients at each position node was then made and used in the following time step. The condition that the surface area be A_m and stress free [eq. (5)] was relaxed during the initial time ($t = 0$) until the penetrant front had moved into the polymer. This was necessary to avoid an infinite gradient in strain at the plate surface. Once the concentration profile had been calculated, the mass uptake was evaluated by an integration (using Simpson's rule) over the plate volume.

Mass Uptake Results

The large number of parameters involved in the model described above required that the value of some of these parameters be set independently if the model was to be useful. Of the eight parameters involved (i.e., μ_m, μ_0, D_m^p, D_0^p, v^p, C_f^p, A_s, and E_c/E_m) the last three were predetermined and fixed. The front concentration, C_f^p, was taken to be the concentration which would bring the glass transition temperature of the plasticized polymer to the temperature of the experiment. This concentration was taken to be $C_f^p = 0.7C_s^p$ based on the results of Andrews et al.[18] The area A_s of the saturated unstressed plate was determined experimentally to be 17% larger than the original plate area. Since the concentration dependence of Young's modulus was not known and E_c/E_m could not be directly determined, this ratio was taken to be in the range suggested by Crank,[2] $E_c/E_m = 5.0$.

The results of the model applied to the three thicknesses, 1/32 in. (0.071 cm), 1/16 in. (0.147 cm), and 1/8 in. (0.318 cm) for the methanol/PMMA system are shown in Figure 5. The procedure was to determine the five remaining parameters of the model by simultaneously fitting the data of both the 1/32-in. and 1/8-in. plates; the parameters that resulted were then used to fit the third plate of 1/16-in. thickness. The agreement is good; and the values of the diffusion coefficients obtained, $D_0^p = 8.79 \times 10^{-10}$ cm^2/sec and $D_m^p = 1.56 \times 10^{-7}$ cm^2/sec, are well within the expected range of values for diffusion coefficients of organic solvents at low and high concentrations, respectively. The value of the front velocity, $v^p = 1.75 \times 10^{-7}$ cm/sec, also compares reasonably well with the value of 3×10^{-6} cm/sec, extracted from the data of Thomas and Windle.[11] However, using the parameters thus determined, the model would predict a critical dry plate minimum thickness of $2L = 0.80$ cm above which all sorption plots would coincide. This is indicated by the dashed curve of Figure 5 which lies much lower than the results of the 1/8-in. (0.318 cm) thick plate which was experimentally found to be on or very close to the limiting curve (see Fig. 2). A second more successful approach was to adjust the parameters such that the predicted limiting curve from the model would be the same as that experimentally observed. This is shown in Figure 6, where the data for the three thickest plates, 1/8 in. (0.318 cm),

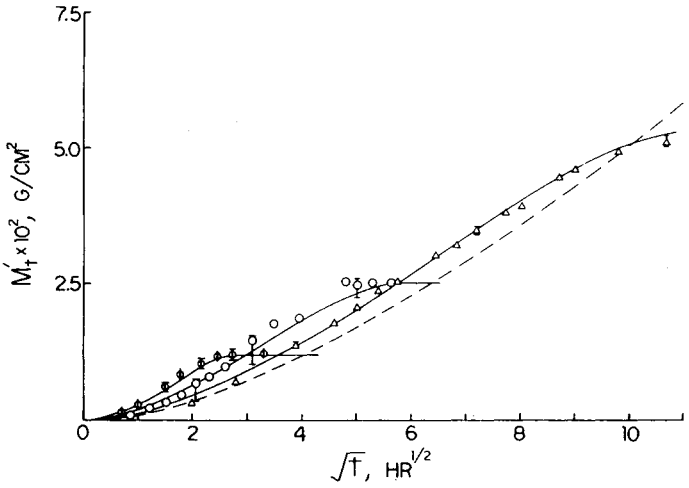

Fig. 5. Comparison of experimental mass uptake data per unit area vs. square root of time for methanol in PMMA at 42°C with calculated curves from the proposed model: $2L$ = 0.071 cm ($1/32$ in.) (ϕ); $2L$ = 0.147 cm ($1/16$ in.) (○); $2L$ = 0.318 cm ($1/8$ in.) (Δ). Fixed model parameters: A_s/A_0 = 1.17, E_c/E_m = 5.0, and C_f^p = 0.203. Parameters fitted: $D_m^p = 1.56 \times 10^{-7}$ cm^2/sec, $D_0^p = 8.79 \times 10^{-10}$ cm^2/sec, $v^p = 1.75 \times 10^{-7}$ cm/sec, μ_m = 7.49, and μ_0 = 25.8. Dashed line represents predicted "limiting" curve, $2L$ = 0.80 cm, according to the parameter values used.

$3/16$ in. (0.476 cm), and $1/4$ in. (0.635 cm) were satisfactorily fitted using the following parameter values: $D_0^p = 1.41 \times 10^{-9}$ cm^2/sec, $D_m^p = 1.07 \times 10^{-7}$ cm^2/sec, $v^p = 2.87 \times 10^{-7}$ cm/sec, μ_0 = 24.1, and μ_m = 7.42. When these values were used on the thinner plates, the predicted behavior was only slightly lower than that experimentally observed, as represented in Figure 6, by the results for the thinnest plate. The important aspect of these results is that all the data were fitted with the *same* set of parameter values, which must depend only on the solvent–polymer system considered and the temperature. A comparison of the

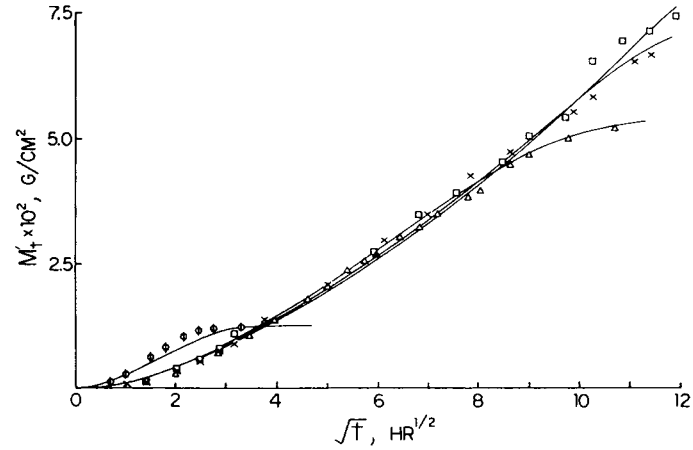

Fig. 6. Comparison of experimental mass uptake data per unit area vs. square root of time for methanol in PMMA at 42°C with calculated curves from the proposed model: $2L$ = 0.071 cm ($1/32$ in.) (ϕ); $2L$ = 0.318 cm ($1/8$ in.) (Δ); $2L$ = 0.476 cm ($3/16$ in.) (×); $2L$ = 0.635 cm ($1/4$ in.) (□). Model parameters fixed: A_s/A_0 = 1.17, E_c/E_m = 5.0, and C_f^p = 0.203. Parameters fitted: $D_m^p = 1.07 \times 10^{-7}$ cm^2/sec, $D_0^p = 1.41 \times 10^{-9}$ cm^2/sec, $v^p = 2.87 \times 10^{-7}$ cm/sec, μ_m = 7.42, and μ_0 = 24.1.

model prediction, using this same set of parameter values, to the experimental results for the 1/32, 1/8, 3/16, and 1/4-in. plates is shown in Figure 7 as a plot of M_t/M_∞ vs. $t^{1/2}/2L$. Sigmoidal, nonsuperimposable sorption curves were obtained for all plate thicknesses; however, the predicted behavior for the thinnest plate was again shown to be lower than that experimentally observed. The important feature displayed by Figure 7 when considered with Figure 6 is that in addition to satisfactorily fitting the mass uptake data for different plate thicknesses with the same set of parameter values, this model reproduces thickness anomalies in both the M_t vs. $t^{1/2}$ and the M_t/M_∞ vs. $t^{1/2}/2L$ sorption plots, unlike any other existing model.

An indication of the sensitivity of the mass uptake plots to the values of D^p and v^p may be conveyed by mentioning that the experimental data of the thinnest plate in Figures 6 and 7 could be matched almost exactly by only changing D_m^p from 1.07×10^{-7} cm^2/sec to 1.70×10^{-7} cm^2/sec and v^p from 2.87×10^{-7} cm/sec to 2.71×10^{-7} cm/sec, keeping all other parameters the same.

Mass uptake kinetics were strongly affected by the value of μ_m. In Figures 5 and 6 the μ_m values had the effect of changing the diffusion coefficient in the swollen region, D_{sw}^p, by a factor of 16 from its value in the fully compressed state to the value just after the fronts meet. This order of magnitude change of D_{sw}^p seems plausible considering the large stresses that are believed to accompany the sorption process. On the other hand, the sorption kinetics were less dependent on μ_0. The values of μ_0 used in Figures 5 and 6 allowed the diffusion coefficient in the glassy core to increase only by a factor of 5 during the sorption process.

Concentration Profiles

Concentration profiles predicted from this model for the 1/32-in. ($2L = 0.071$ cm) plate are presented in Figure 8. The values of the parameters used in calculating these curves were those resulting from the fit of the 1/8, 3/16, and 1/4-in. plates. Shown are concentration profiles in both the polymer frame of reference, ξ, and the lab frame, x. The transformation of the concentration profile obtained from eq. (2) to the lab frame of reference is discussed in the Appendix. The use

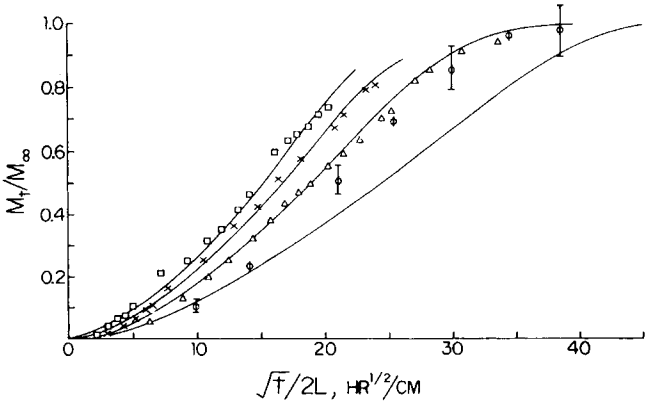

Fig. 7. Comparison of experimental sorption curves for methanol in PMMA at 42°C with calculated curves from proposed model. Symbols and model parameters are those of Figure 6.

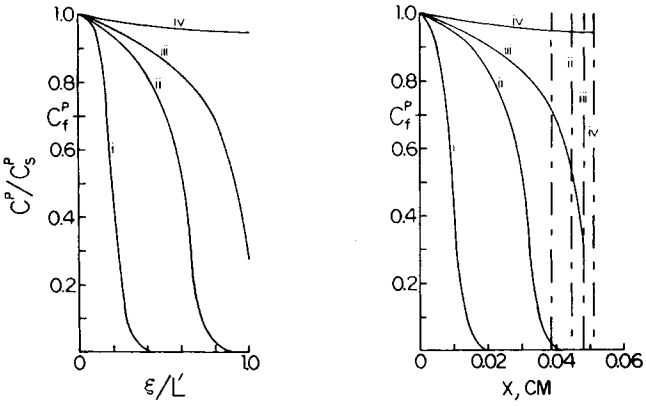

Fig. 8. Calculated concentration profiles for methanol in the 1/32-in. ($2L$ = 0.071 cm) PMMA plate in ξ and x frames of reference at successive times. Dashed vertical lines in the x frame of reference correspond to model prediction of the plate center line at given times. Model parameters used correspond to those of Figure 6; (i) t = 0.88 hr, (ii) t = 3.6 hr, (iii) t = 6.2 hr, and (iv) t = 8.8 hr.

of a step function for the concentration dependence of the diffusion coefficient in the swollen and glassy regions has resulted in the sharpest concentration profiles obtainable. The degree of sharpness in the concentration profile varies with the location of the diffusion coefficient discontinuity which depends on the value of the arbitrary concentration, C_f^p. As seen in Figure 8, a relatively sharp front is predicted to penetrate into the polymer as time proceeds, leaving a substantial portion of the polymer behind the front near the saturation concentration. Once the fronts have met, a smoother concentration distribution exists in the polymer. This sharp advancing concentration profile and the discontinuity in the slope at the center line as the fronts meet are qualitative features that have been observed experimentally for the methanol/PMMA system by Thomas and Windle.[11] Figure 8 also shows the effect of considering polymer swelling by the penetrant. The dashed vertical lines in the lab frame of reference plot represent the model prediction of the plate center line and show how the plate increases in thickness at successive times.

CONCLUSIONS

Experimental results of the "anomalous" diffusion of methanol in poly(methyl methacrylate) cannot be explained in terms of a combination of the two limiting cases of sorption, Fickian diffusion, and case II mechanism. In the range of plate thickness examined here, strain effects on the diffusion coefficient appear to be affecting the sorption process in addition to the stress gradient contribution to the flux. We have presented a model where strain effects on the diffusion coefficient are obtained in a manner consistent with the stress contribution to the flux. In view of the approximations built in our model due to our simplifying assumptions of the strain dependence of the diffusion coefficient and given the unsophistication of mass uptake experiments, the proposed model seems to successfully account for the diffusion anomalies in the methanol/PMMA system. These anomalies are characterized by sorption curves that are sigmoidal in shape and thickness dependent, and by faster mass uptake rates per unit area for thinner plates below a limiting thickness. The model also reproduces the qualitative features of the concentration profiles.

The PMMA plate dimensions used for these experiments were scaled so that the plate edge effects could be neglected from a mass transfer point of view, i.e., the plates were assumed to be infinite in the lateral directions. It has yet to be demonstrated whether or not this same scaling is the correct one to use when strains are present in the plates. Since the three thickest plates, 1/8, 3/16, and 1/4 in., did not display a significant strain effect on the diffusion coefficients, it would seem that increasing the plate area of these samples would not alter the sorption characteristics; however, it has not been determined whether or not increasing the area of the 1/32-in. plate would significantly affect the strain within the polymer and the subsequent mass uptake kinetics. This scaling of plates from a strain aspect is an important point which needs further attention for a fuller understanding of the strain influence on the diffusion coefficient.

This work was supported in part by a Young Faculty du Pont Grant and in part by an NSF Grant, Polymers Program, DMR 7815738.

APPENDIX

The concentration profile obtained in terms of ξ and t can easily be transformed back into the lab coordinate, x, by use of the relation between the lab and polymer frames of reference[17]

$$d\xi = \phi_p \, dx \tag{A-1}$$

where ϕ_p is the polymer volume fraction. The use of this transformation involves the assumption of additive volumes of the polymer and penetrant. With this approximation, the concentration in the polymer frame of reference can be written as

$$C^p = \frac{\rho_s \phi_s}{\rho_p \phi_p} = \frac{\rho_s \phi_s}{\rho_p (1 - \phi_s)} \tag{A-2}$$

where ρ_s and ϕ_s are the density and volume fraction of the swelling agent and ρ_p and ϕ_p are the corresponding quantities for the polymer. From eq. (A-2) one obtains

$$\phi_s = \frac{C^p}{\rho_s/\rho_p + C^p} \tag{A-3}$$

which, when substituted into eq. (A-1) and noting that $\phi_p = 1 - \phi_s$, gives after simplification

$$d\xi = \frac{\rho_s}{\rho_s + \rho_p C^p} dx \tag{A-4}$$

Hence the concentration at a point ξ in the polymer frame of reference corresponds to the concentration at the point x in the lab frame where x is obtained from the relation

$$x = \int_0^\xi \left(1 + \frac{\rho_p}{\rho_s} C^p\right) d\xi \tag{A-5}$$

Note that C^p is a function of ξ determined by eq. (2).

References

1. J. H. Petropoulos, and P. P. Roussis, in *Permeability of Plastic Films and Coatings to Gases, Vapors, and Liquids*, H. B. Hopfenberg, Ed., Plenum, New York, 1974, p. 219.
2. J. Crank, *J. Polym. Sci.* **11**, 151 (1953).
3. L. Mandelkern and F. Long, *J. Polym. Sci.*, **6**, 457 (1951).
4. G. S. Park, *J. Polym. Sci.*, **11**, 97 (1953).
5. T. Alfrey, Jr., E. F. Gurnee, and W. O. Lloyd, *J. Polym. Sci., Polym. Symp.*, **12**, 249 (1966).
6. H. L. Frisch, T. T. Wang, and T. K. Kwei, *J. Polym. Sci., Part A*, **7**, 879 (1969).
7. T. T. Wang, T. K. Kwei, and H. L. Frisch, *J. Polym. Sci., Part A*, **7**, 2019 (1969).
8. D. J. Enscore, H. B. Hopfenberg, and V. T. Stannett, *Polymer*, **18**, 793 (1977).
9. A. R. Berens and H. B. Hopfenberg, *Polymer*, **19**, 489 (1978).
10. F. A. Long and D. Richman, *J. Am. Chem. Soc.*, **82**, 513 (1960).

11. N. L. Thomas and A. H. Windle, *Polymer,* **19,** 255 (1978).
12. A. S. Michaels, H. J. Bixler, and H. B. Hopfenberg, *J. Appl. Polym. Sci.,* **12,** 991 (1968).
13. Plexiglas Design and Fabrication Data, PL-229n, Rohm and Haas Company, January 1976.
14. T. T. Wang and T. K. Kwei, *Macromolecules,* **6,** 919 (1973).
15. T. K. Kwei, T. T. Wang, and H. M. Zupko, *Macromolecules,* **5,** 645 (1972).
16. J. H. Petropoulos and P. P. Roussis, *J. Membr. Sci.,* **3,** 343 (1978).
17. G. S. Hartley and J. Crank, *Trans. Faraday Soc.,* **45,** 801 (1949).
18. E. H. Andrews, G. M. Levy, and J. Willis, *J. Mater. Sci.,* **8,** 1000 (1973).

Received September 13, 1979